

Validation and application of soil moisture active passive sea surface salinity observation over the Changjiang River Estuary

Qiong Wu¹, Xiaochun Wang^{2, 3*}, Wenhao Liang², Wenjun Zhang¹

¹School of Atmospheric Science, Nanjing University of Information Science and Technology, Nanjing 210044, China

²School of Marine Science, Nanjing University of Information Science and Technology, Nanjing 210044, China

³Joint Institute for Regional Earth System Science and Engineering, University of California at Los Angeles, Los Angeles 90095, USA

Received 19 April 2019; accepted 27 May 2019

© Chinese Society for Oceanography and Springer-Verlag GmbH Germany, part of Springer Nature 2020

Abstract

Using sea surface salinity (SSS) observation from the soil moisture active passive (SMAP) mission, we analyzed the spatial distribution and seasonal variation of SSS around Changjiang River (Yangtze River) Estuary for the period of September 2015 to August 2018. First, we found that the SSS from SMAP is more accurate than soil moisture and ocean salinity (SMOS) mission observation when comparing with the *in situ* observations. Then, the SSS signature of the Changjiang River freshwater was analyzed using SMAP data and the river discharge data from the Datong hydrological station. The results show that the SSS around the Changjiang River Estuary is significantly lower than that of the open ocean, and shows significant seasonal variation. The minimum value of SSS appears in July and maximum SSS in December. The root mean square difference of daily SSS between SMAP observation and *in situ* observation is around 3 in both summer and winter, which is much lower than the annual range of SSS variation. In summer, the diffusion direction of the Changjiang River freshwater depicted by SSS from SMAP is consistent with the path of freshwater from *in situ* observation, suggesting that SMAP observation may be used in coastal seas in monitoring the diffusion and advection of freshwater discharge.

Key words: soil moisture active passive mission, *in situ* observation, soil moisture and ocean salinity mission, sea surface salinity, Changjiang River (Yangtze River) Estuary, freshwater plume

Citation: Wu Qiong, Wang Xiaochun, Liang Wenhao, Zhang Wenjun. 2020. Validation and application of soil moisture active passive sea surface salinity observation over the Changjiang River Estuary. *Acta Oceanologica Sinica*, 39(4): 1–8, doi: 10.1007/s13131-020-1542-z

1 Introduction

Sea surface salinity (SSS) can be considered as an indicator of the water cycle and the flux of freshwater across the air sea interface (Bingham et al., 2011). The low SSS areas are usually occupied by precipitation, freshwater and melting glaciers (Dickson et al., 1988; Durack and Wijffels, 2010). Currently, the main methods for obtaining SSS are *in situ* observation and satellite remote sensing (Bai et al., 2013, 2014).

In situ observations are widely used for scientific researches and ocean operational monitoring. The temperature and salinity from Argo profiles are often utilized to address the seasonal and interannual variability of SSS of many regions, such as the eastern Equatorial Indian Ocean and Southeastern Arabian Sea (Subrahmanyam et al., 2011). Liu and Feng (2012) studied the salinity data, which were collected on two zonal sections near the Jeju Island, to analyze the impact of wind on the transport of the Changjiang River freshwater plume in August. However, the *in situ* observation cannot describe the variations of SSS at finer spatial and temporal scales. Increasing availability of the satellite observations of SSS data will undoubtedly provide us with more accurate method to observe SSS. At present, several satellites such as AQUARIUS, SMOS and SMAP have been launched for observing SSS. SMOS is the first satellite mission to address the

challenge of measuring SSS from space by the European Space Agency in 2009 (Berger et al., 2002; Font et al., 2010). Hasson et al. (2018) and Guimbard et al. (2017) analyzed the 2015–2016 El Niño event with SSS from SMOS, found that the SSS is strong anomalies in the tropical Pacific. AQUARIUS is launched for observing the SSS from space with a combined passive/active L-band microwave instrument in 2011. The SSS data supports us to investigate the coupling relationships between ocean circulation, global water cycle, and climate (Le Vine et al., 2007; Lagerloef et al., 2008; Yueh et al., 2014). The SMAP mission is one of the first Earth observation satellites of National Aeronautics and Space Administration (NASA) to detect soil moisture from January of 2015. The SMAP can distinguish frozen from thawed land surfaces, it improving the estimates of water, energy, and carbon transfers between the land and the atmosphere. The SMAP mission provides high resolution and high accuracy soil moisture and frozen/thaw state data using L-band radar and radiometer instruments (Entekhabi et al., 2010, 2014; Das et al., 2011; Yueh et al., 2016). The SMAP can directly exhibit the flood assessment and drought monitoring of many large rivers through the distributions of SSS observations, such as the Niger River, the Amazon River, the Nujiang River, the Mississippi River and the Ganges River (Yueh et al., 2016). The SSS from SMAP was used to focus

Foundation item: The National Key Research and Development Program of China under contract No. 2016YFC1401600; the Public Science and Technology Research Fund Projects for Ocean Research under contract No. 201505003; the 2015 Jiangsu Program of Entrepreneurship and Innovation Group under contract No. 2191061503801/002.

*Corresponding author, E-mail: xcwang@nuist.edu.cn

on the May 2015 severe flooding in Texas (Fournier et al., 2016).

SSS satellite missions provide new opportunities to study SSS variation and their potential applications in terms of ocean monitoring and forecasting need to be explored, especially in coastal regions where the riverine freshwater discharge plays a significant role in oceanic processes and *in situ* salinity observation is often sparse in space. In present research, the SSS observation from SMAP mission is used to study SSS variation around Changjiang River Estuary. Section 2 introduces the materials we used in the study. Section 3 validates SMAP and SMOS observations using *in situ* observation and analyzes SSS variability of SMAP on seasonal and sub-seasonal time scales. In section 4, we summarize results.

2 Data

In present study, the SMAP data we used is from September 1, 2015 to August 31, 2018 while the SMOS data is from September 1, 2015 to August 31, 2016. The SMAP is a gridded product with 1-day temporal resolution and 0.25° horizontal resolution while the temporal resolution of SMOS is 4-day and the spatial resolution is 0.26°.

The *in situ* measurement of sea-bird SBE CTD used for all measurements is from the R/V *Rongjiang No. 1*. The two observation time periods are from December 20 to 30, 2015 and August 3 to 13, 2016. For each station, the CTD instrument is put in the water for 3–5 min, and descends with a speed around 1 m/s. The procedure was repeated 1–2 times to measure temperature and salinity. Our data quality control procedure includes two steps.

First, we removed all the data with the pressures smaller than 0. Second, the temperature and salinity with variability larger than 3 standard deviations are removed.

The daily freshwater discharge data of the Datong hydrological station over the Changjiang River from September 2015 to August 2018 is used in this study (<http://xxfb.hydroinfo.gov.cn>).

3 Results

3.1 Comparisons of SSS from satellite datasets with *in situ* observations

In this study, the SSS obtained from SMAP and SMOS satellite datasets were used to validate against *in situ* SSS observations over the Changjiang River Estuary. The scatter plot of Fig. 1 shows the SSS of SMAP observation (Figs 1a, b) and *in situ* observation between winter, 2015 (Figs 1a, c) and summer, 2016 (Figs 1b, d) while the SMOS observations are shown in Figs 1c and d. The RMSD between the *in situ* observation and SMAP is 3.15, with the bias of -1.36 in winter 2015. The RMSD is 2.79 with -0.63 bias between *in situ* observation and SMOS. From above comparisons, we found that both the SMAP and SMOS overestimated SSS. However, the quality of SMOS SSS is slightly better than SMAP in winter. The RMSD between the *in situ* observation and SMAP is 3.02, with the bias of 0.47 in summer. The RMSD of the *in situ* observation and SMOS is 3.95 with the bias of 0.54, which means that the SMAP mission and SMOS mission both overestimated SSS during summer. However, the error of SMAP observation is smaller than SMOS.

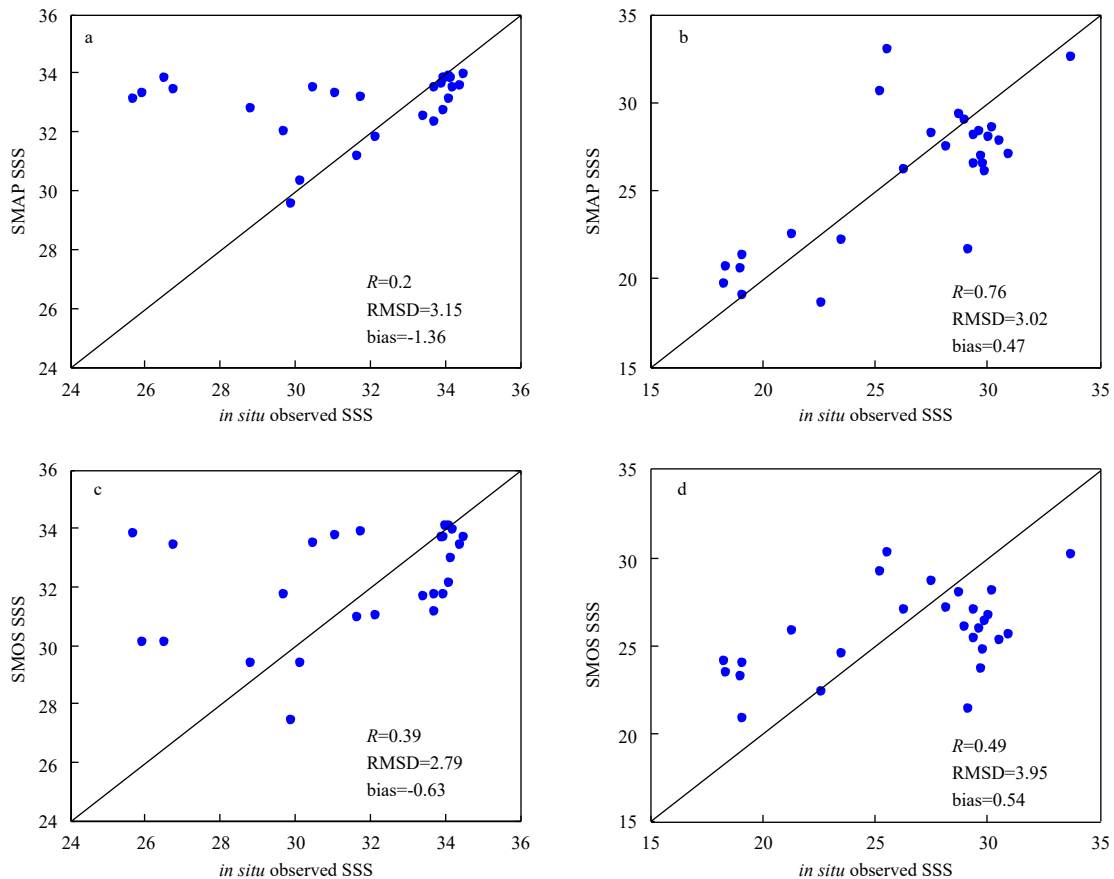


Fig. 1. Comparison of SSS data from SMAP and SMOS missions against *in situ* observations. a. The correlation coefficient (R), root mean square difference (RMSD) and bias between SMAP data and *in situ* observation in winter of 2015, b. the same as a but for summer of 2016, c. the same as a but for SMOS dataset, and d. the same as b but for SMOS dataset.

Though there is large bias of SMAP SSS observation during the winter of 2015, it is encouraging to note the similarity between SSS spatial distribution from SMAP (Fig. 2a) and *in situ* measurement (Fig. 2b). For instance, gradual increase of SSS from around 29 to 31 along 32°N is visible in both SMAP and *in situ* SSS observation. Figures 2c and d present the distribution of SMAP and *in situ* CTD observation for the summer of 2016. The major feature in both SMAP and *in situ* SSS observation is the northeastward extension of Changjiang River freshwater plume, similar to the observations of Kim et al. (1991) and Xuan et al. (2012). Though the RMSDs in SMAP SSS observation are as large as 3, it is encouraging to note that the SMAP SSS observation has great potential to monitor the spreading of freshwater plume from the Changjiang River.

Similar to the validation of SMAP SSS against *in situ* observation, the SSS spatial distribution derived from SMOS data also shows consistent distribution with that of the *in situ* SSS observation (Fig. 3). Along 32°N, the SSS from both SMOS and *in situ* observation increase from around 29 to 31. Figures 3c and d present

the spatial distributions of the SMOS SSS and *in situ* observation in summer of 2016. Although the SSS of the SMOS observation reproduces the main characteristics of the Changjiang River freshwater that extends to the northeast, the value of the SMOS SSS is larger than that of the *in situ* SSS observation, especially over the stations (C1 to C7) region. During summer of 2016, SMOS SSS has a larger bias and RMSD than those of SMAP SSS (Figs 1b, d). Thus, in the following analysis, we only use SMAP SSS.

3.2 Annual mean and variation of SSS

Due to the sparseness of *in situ* observations, the fine spatial SSS distribution is still unclear over the Changjiang River Estuary according to previous studies. However, the SSS observations from satellites have shown great potential based on the validation of SSS from satellites (SMAP and SMOS) against *in situ* observation in this study. The SMAP SSS observation can better represent the spatial distribution of SSS over the Changjiang River Estuary. Figure 4a shows annual mean SMAP SSS averaged from previous September to next August during the period of 2015–

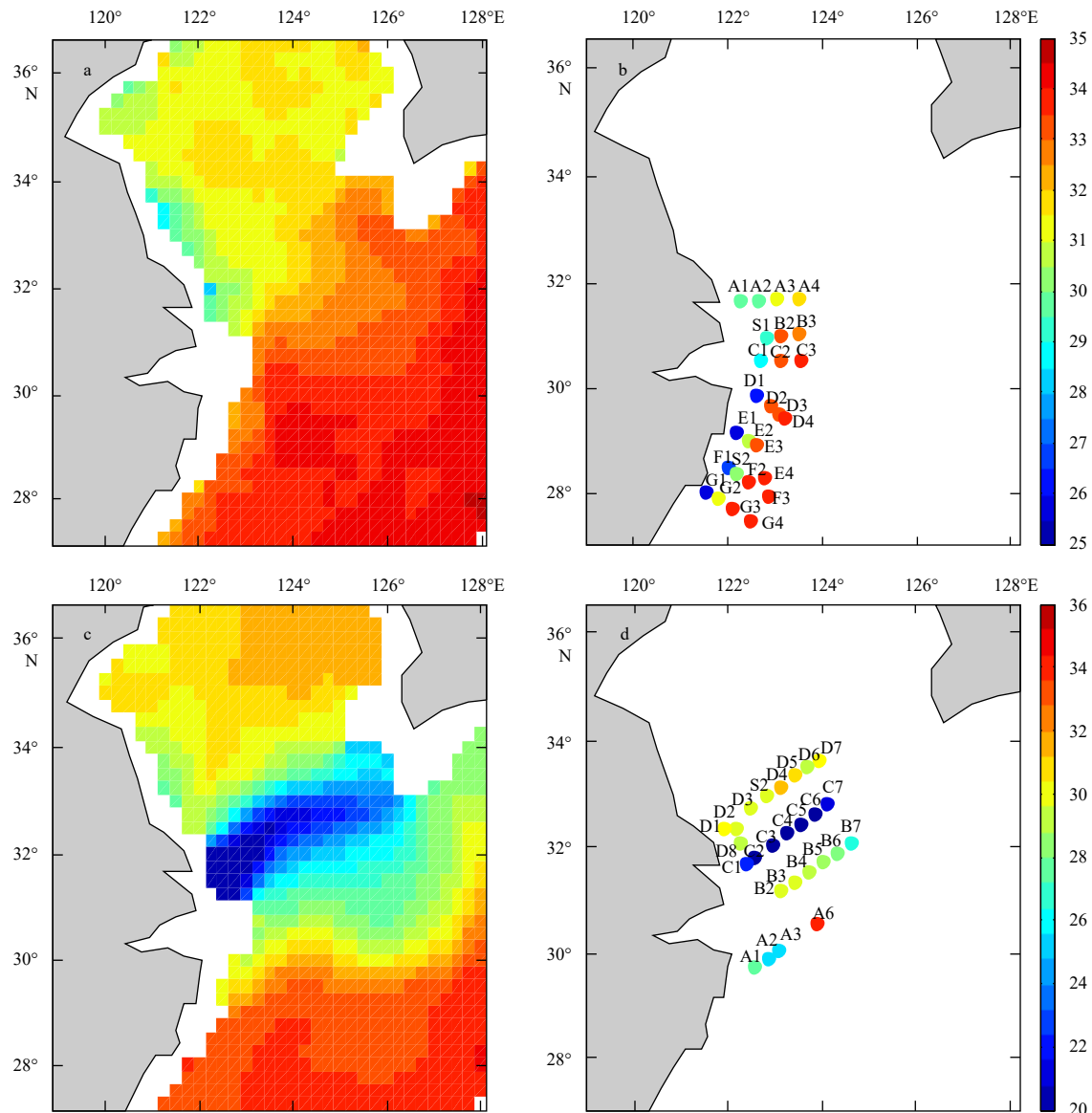


Fig. 2. SSS of SMAP during December 20–30, 2015 (a); SSS of *in situ* CTD observation during December 20–30, 2015 (b); SSS of SMAP during August 3–13, 2016 (c); and SSS of *in situ* CTD observation during August 3–13, 2016 (d).

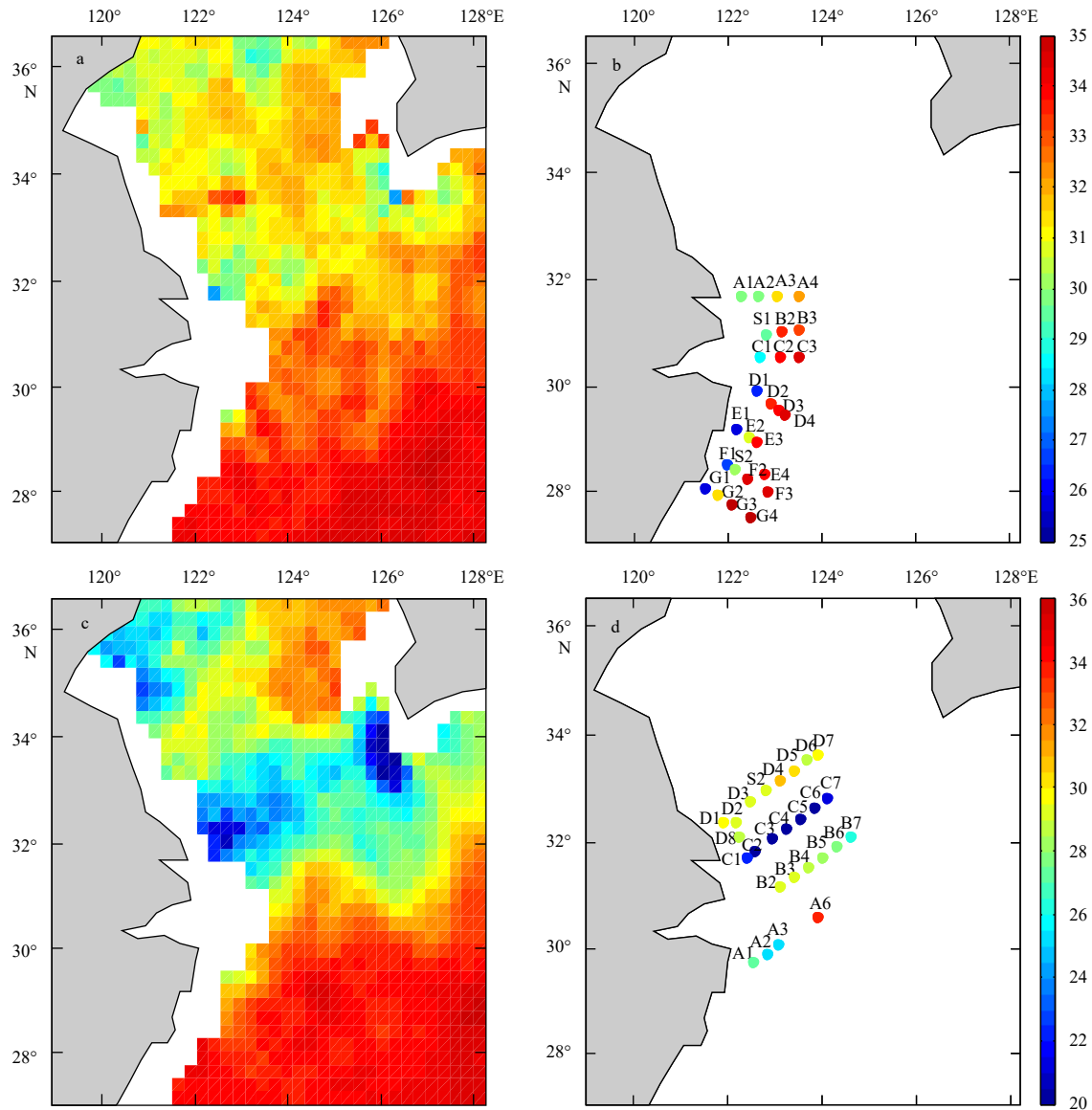


Fig. 3. SSS from SMOS observation in December 20–30, 2015 (a); SSS from *in situ* observation in December 20–30, 2015 (b); SMOS SSS observation in August 4–12, 2016 (c); and *in situ* SSS observation in August 3–13, 2016 (d).

2018 over the Changjiang River Estuary. Owing to the effect of large freshwater, the minimum value of annual mean SSS around the Changjiang River Estuary is close to 25. We further describe the spatial variation of the SSS value over the Changjiang River Estuary by calculating the difference between the highest and lowest values of the SSS at each grid point, as shown in Fig. 4b. An important characteristic of the SSS is that it decreased sharply from the near shore area to the offshore area. The range of SSS around the Changjiang River Estuary can reach as high as 16.

3.3 Seasonal variation

Figures 5a–l show seasonal evolutions of SSS during the period of 2015–2018. The value of the SSS ranges from 29 to 34 from previous September to next August over the Changjiang River Estuary. Figures 5a–d display that the low SSS region over the Changjiang River Estuary gradually decays from September to December. Figures 5e–l indicate that the low value SSS region gradually extends from coastal regions to outer sea from January to August. Because of the gradual increase of precipitation over

the middle and lower reaches of the Changjiang River from previous winter to next summer, the SSS reaches the maximum in December (Fig. 5d) while it reaches the minimum in July (Fig. 5k).

The averaged SSS over the region (32°–33°N, 122°–124°E) is used as an indicator of the Changjiang River Estuary for analyzing the relationship between SSS variation and hydrological cycle. Figure 6 displays the time series of mean SSS and mean freshwater discharge during the same period. The freshwater discharge ranges from 2×10^4 to 3×10^4 m³/s from September to February, and the SSS gradually increases from 30 to around 32. The SSS sharply decreased from May to August, reaching a minimum value of 26 in August, while the discharge value increased gradually and reached peak (7×10^4 m³/s) in July. In general, the averaged SSS and freshwater discharge has a significant negative correlation. Large freshwater discharge corresponds to the low SSS and the small freshwater discharge is consistent with the high SSS over the Changjiang River Estuary. The correlation coefficient between mean SSS and freshwater discharge is -0.89 which is significant at the 95% confidence level.

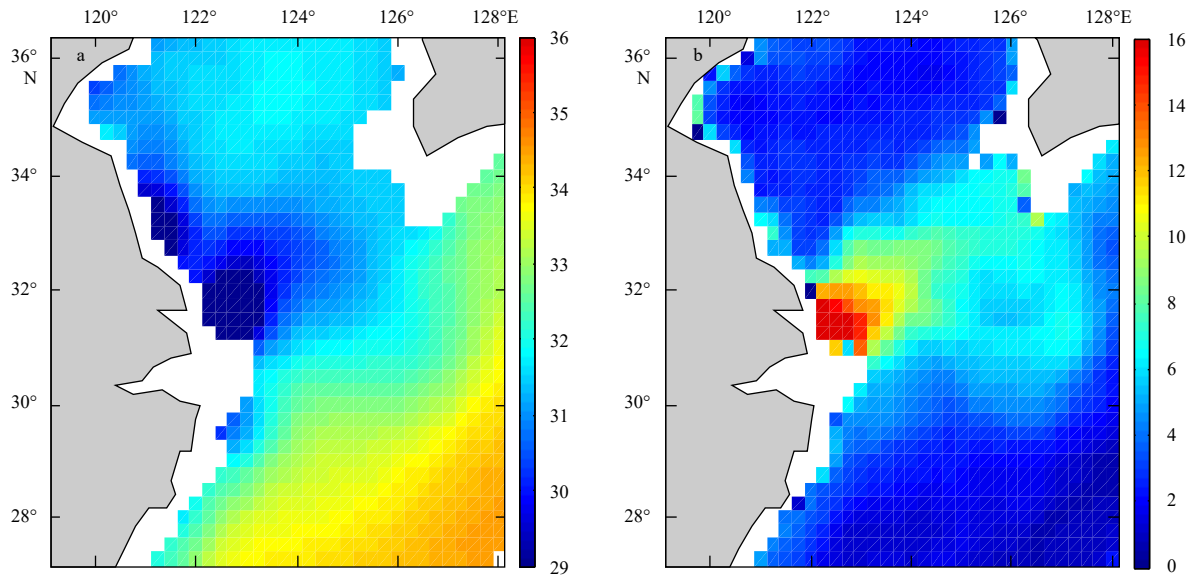


Fig. 4. Annual mean SMAP SSS averaged from previous September to next August during the period of 2015–2018 over the Changjiang River Estuary (a); and the spatial distribution of the range of SSS, the difference between the highest and the lowest SSS for each point (b).

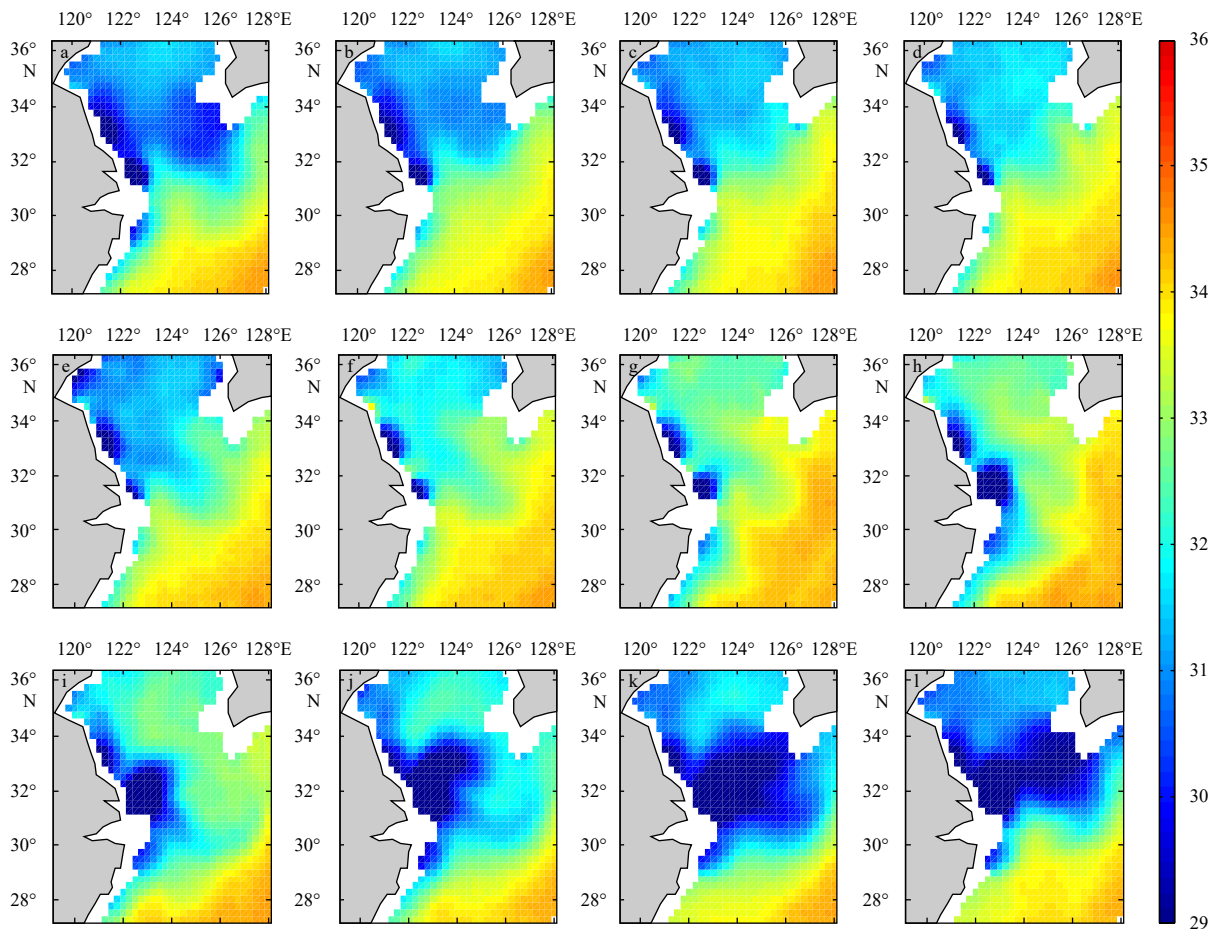


Fig. 5. Seasonal evolutions of SSS from previous September to next August (3-year averaged from 2015–2018) of the Changjiang River Estuary.

3.4 Path of the Changjiang River freshwater discharge

Owing to the advantages of SMAP data in terms of high spa-

tial and temporal resolution, we can investigate the spread of river plume from the near shore area to the offshore area. A signi-

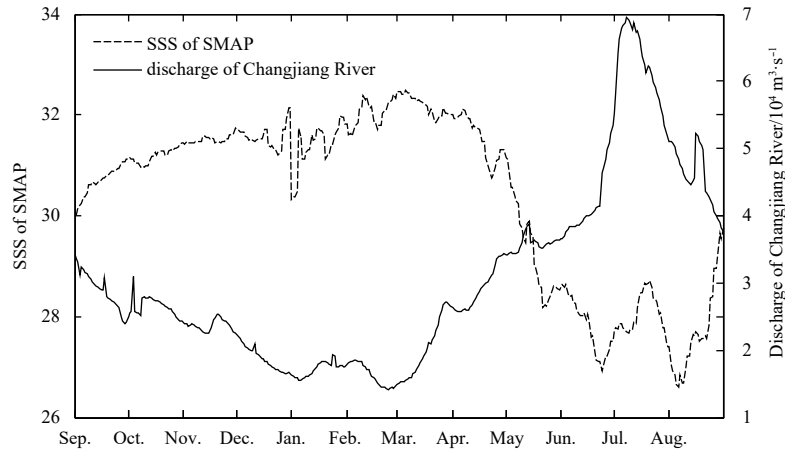


Fig. 6. The time series of SSS averaged over the region (32° – 33° N, 122° – 124° E) and the freshwater discharge of the Datong hydrological station from previous September to next August (3-year averaged from 2015–2018). The unit of discharge is m^3/s .

ficant characteristic of the diffusion of the Changjiang River discharge is that it spreads northeastward from May to July while this trend of northeastward extension weakens in August (Fig. 5). Figures 7a–f show the SSS spatial evolution from May to July with 15-day interval averaged from 2015 to 2018. The low SSS area expands northeastward gradually, with the increasing freshwater discharge of the Changjiang River from May to July.

The diffusion path of the Changjiang River freshwater during winter is completely different from that during summer. Figures 8a–f show the evolution of SSS from December to February with 15-day temporal interval. The SSS gradually increases along the coastal area from 30° N to the south (Mao et al., 1963), indicating that the freshwater plume is weak and spreads southward along the coast. The diffusion path may be related to the north wind in winter. Overall, the area of freshwater diffusion in winter is much smaller than that in summer. Besides the discharge, wind is also

an important factor that cannot be ignored. Due to the influence of monsoon system, the southwesterly wind prevails in summer, leading to the extension of the low SSS area northeastward. However, the winter is dominated by the northeasterly wind, and the low SSS region extends to the southwest. Based on Figs 7 and 8, we can draw a conclusion that due to the different value of discharge and the direction of wind, the scope and direction of the Changjiang River freshwater diffusion are far different at seasonal time scales. Though these features were analyzed using *in situ* data in previous studies, our analysis demonstrates the potential to use satellite SSS data to study and even monitor the spreading of the Changjiang River freshwater.

4 Conclusions

In this study, we compare SSS from SMAP and SMOS missions, with *in situ* observation, and find that the RMSDs between

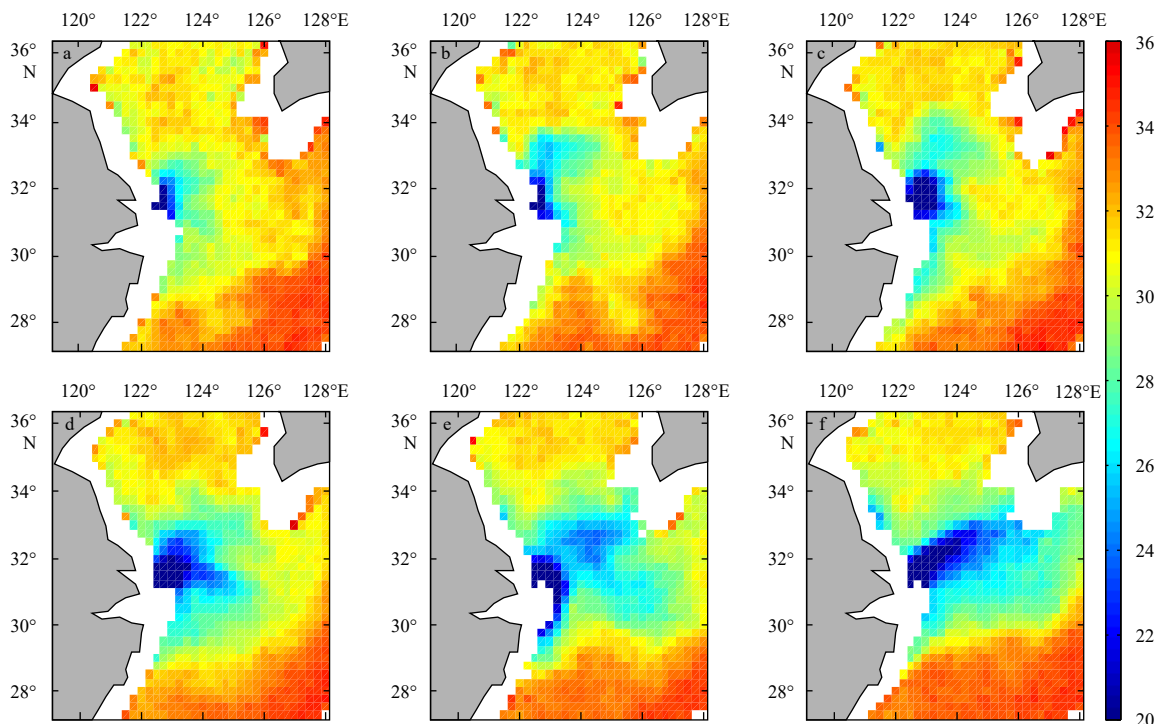


Fig. 7. The SSS evolutions from May to July with 15-day intervals over the Changjiang River Estuary averaged from 2015–2018.

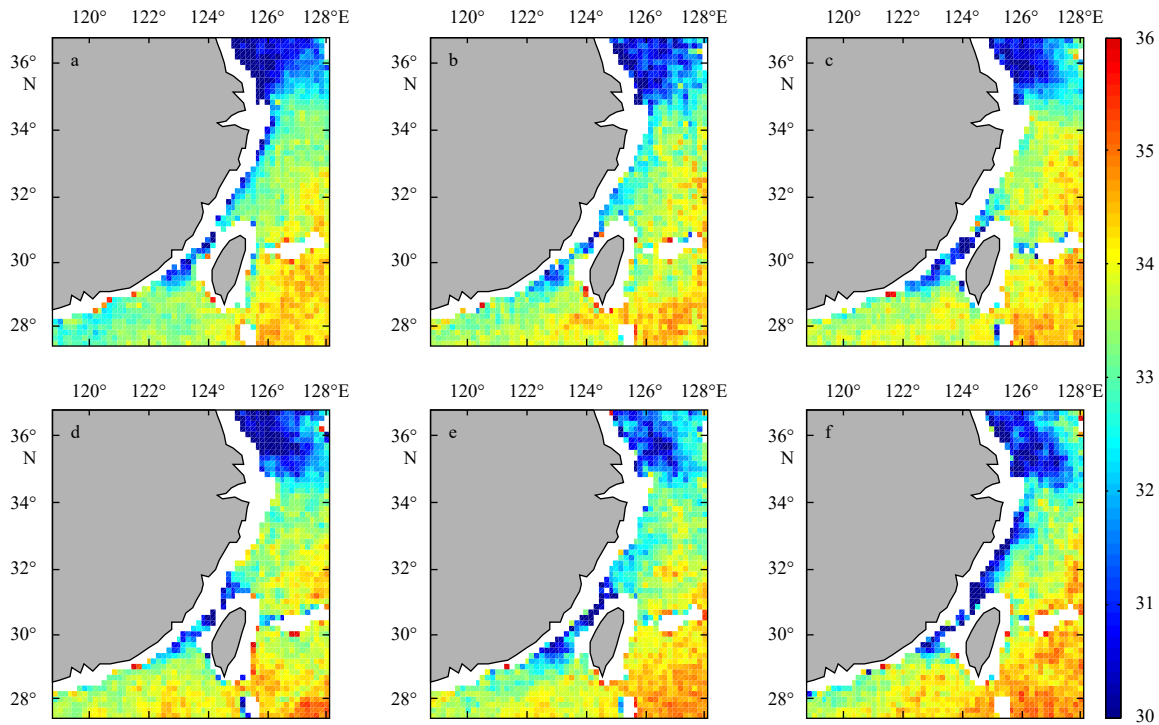


Fig. 8. The SSS evolution from previous December to February of next year with 15-day intervals for the Changjiang River Estuary averaged from 2015–2018.

satellite SSS and *in situ* observations are about 3. However, the SSS derived from SMAP mission may be more suitable for describing the spreading of the freshwater plume from the Changjiang River than SMOS, especially in summer, since SMOS SSS has a larger bias and RMSD than that of SMAP. In addition, we also analyze the spatial distribution and temporal evolutions of SSS around the Changjiang River Estuary using SMAP data. The results show that the SMAP SSS has obvious seasonal cycle. The annual range of SSS, the difference between the maximum value in winter and minimum value in summer, exceeds 16. The averaged SSS over the region (32°–33°N, 122°–124°E) is negatively related with freshwater discharge from the Changjiang River. The Changjiang River freshwater spreads northeastward during summer time and southwestward during winter time. Our analysis demonstrates the potential of satellite SSS for studying and monitoring the Changjiang River freshwater plume in the East China Sea.

Acknowledgements

We thank Xianqiang He and the crew member of R/V *Rongjiang No. 1* for making *in situ* CTD observations in the winter of 2015, and summer of 2016. The SMAP data are downloaded from the National Snow and Ice Data Center (NSIDC, <http://nsidc.org/the-drift/data-set/smap/>).

References

- Bai Yan, He Xianqiang, Pan Delu, et al. 2014. Summertime Changjiang River plume variation during 1998–2010. *Journal of Geophysical Research: Oceans*, 119(9): 6238–6257, doi: [10.1002/2014JC009866](https://doi.org/10.1002/2014JC009866)
- Bai Yan, Pan Delu, Cai Wenjun, et al. 2013. Remote sensing of salinity from satellite-derived CDOM in the Changjiang River dominated East China Sea. *Journal of Geophysical Research: Oceans*, 118(1): 227–243, doi: [10.1029/2012JC008467](https://doi.org/10.1029/2012JC008467)
- Berger M, Camps A, Font J, et al. 2002. Measuring ocean salinity with ESA's SMOS mission- advancing the science. *ESA Bulletin-European Space Agency*, (111): 113–121
- Bingham F M, Foltz G R, McPhaden M J. 2011. Characteristics of the seasonal cycle of surface layer salinity in the global ocean. *Ocean Science Discussions*, 8(6): 2377–2415, doi: [10.5194/osd-8-2377-2011](https://doi.org/10.5194/osd-8-2377-2011)
- Das N N, Entekhabi D, Njoku E G. 2011. An algorithm for merging SMAP radiometer and radar data for high-resolution soil-moisture retrieval. *IEEE Transactions on Geoscience and Remote Sensing*, 49(5): 1504–1512, doi: [10.1109/TGRS.2010.2089526](https://doi.org/10.1109/TGRS.2010.2089526)
- Dickson R R, Meincke J, Malmberg S A, et al. 1988. The “great salinity anomaly” in the northern North Atlantic 1968–1982. *Progress in Oceanography*, 20(2): 103–151, doi: [10.1016/0079-6611\(88\)90049-3](https://doi.org/10.1016/0079-6611(88)90049-3)
- Durack P J, Wijffels S E. 2010. Fifty-year trends in global ocean salinities and their relationship to broad-scale warming. *Journal of Climate*, 23(16): 4342–4362, doi: [10.1175/2010JCLI3377.1](https://doi.org/10.1175/2010JCLI3377.1)
- Entekhabi D, Das N, Yueh S, et al. 2014. SMAP Handbook Soil Moisture Active Passive: Mapping Soil Moisture and Freeze/Thaw from Space. Pasadena, CA: JPL Publication, 31–46
- Entekhabi D, Njoku E G, O'Neill P E, et al. 2010. The soil moisture active passive (SMAP) mission. *Proceedings of the IEEE*, 98(5): 704–716, doi: [10.1109/JPROC.2010.2043918](https://doi.org/10.1109/JPROC.2010.2043918)
- Font J, Camps A, Borges A, et al. 2010. SMOS: the challenging sea surface salinity measurement from space. *Proceedings of the IEEE*, 98(5): 649–665, doi: [10.1109/JPROC.2009.2033096](https://doi.org/10.1109/JPROC.2009.2033096)
- Fournier S, Reager J T, Lee T, et al. 2016. SMAP observes flooding from land to sea: the Texas event of 2015. *Geophysical Research Letters*, 43(19): 10338–10346, doi: [10.1002/2016GL070821](https://doi.org/10.1002/2016GL070821)
- Guimbar S, Reul N, Chapron B, et al. 2017. Seasonal and interannual variability of the Eastern Tropical Pacific Fresh Pool. *Journal of Geophysical Research: Oceans*, 122(3): 1749–1771, doi: [10.1002/2016JC012130](https://doi.org/10.1002/2016JC012130)
- Hasson A, Puy M, Boutin J, et al. 2018. Northward pathway across the tropical North Pacific Ocean revealed by surface salinity: how do El Niño anomalies reach Hawaii?. *Journal of Geophysical Research: Oceans*, 123(4): 2697–2715, doi: [10.1002/2017JC013423](https://doi.org/10.1002/2017JC013423)

- Kim K, Kim K R, Rhee T S, et al. 1991. Identification of water masses in the Yellow Sea and the East China Sea by cluster analysis. *Elsevier Oceanography Series*, 54: 253–267, doi: [10.1016/S0422-9894\(08\)70100-4](https://doi.org/10.1016/S0422-9894(08)70100-4)
- Lagerloef G, Colomb F R, Le Vine D, et al. 2008. The Aquarius/SAC-D mission: designed to meet the salinity remote-sensing challenge. *Oceanography*, 21(1): 68–81, doi: [10.5670/oceanog.2008.68](https://doi.org/10.5670/oceanog.2008.68)
- Le Vine D M, Lagerloef G S E, Colomb F R, et al. 2007. Aquarius: an instrument to monitor sea surface salinity from space. *IEEE Transactions on Geoscience and Remote Sensing*, 45(7): 2040–2050, doi: [10.1109/TGRS.2007.898092](https://doi.org/10.1109/TGRS.2007.898092)
- Liu Baochao, Feng Licheng. 2012. An observational analysis of the relationship between wind and the expansion of the Changjiang River diluted water during summer. *Atmospheric and Oceanic Science Letters*, 5(5): 384–388, doi: [10.1080/16742834.2012.11447027](https://doi.org/10.1080/16742834.2012.11447027)
- Mao H L, Kan T C, Lan Shufang. 1963. A preliminary study of the Yangtze diluted water and its mixing processes. *Oceanologia et Limnologia Sinica* (in Chinese), 5(3): 183–206
- Subrahmanyam B, Murty V S N, Heffner D M. 2011. Sea surface salinity variability in the tropical Indian Ocean. *Remote Sensing of Environment*, 115(3): 944–956, doi: [10.1016/j.rse.2010.12.004](https://doi.org/10.1016/j.rse.2010.12.004)
- Xuan Jiliang, Huang Daji, Zhou Feng, et al. 2012. The role of wind on the detachment of low salinity water in the Changjiang Estuary in summer. *Journal of Geophysical Research: Oceans*, 117(C10): C10004, doi: [10.1029/2012jc008121](https://doi.org/10.1029/2012jc008121)
- Yueh S, Fore A, Tang Wenqing, et al. 2016. Applications of SMAP data to retrieval of ocean surface wind and salinity. In: *Proceedings of SPIE 9999, Remote Sensing of the Ocean, Sea Ice, Coastal Waters, and Large Water Regions 2016*. Edinburgh, United Kingdom: SPIE, doi: [10.1117/12.2240710](https://doi.org/10.1117/12.2240710)
- Yueh S, Tang Wenqing, Fore A, et al. 2014. Aquarius geophysical model function and combined active passive algorithm for ocean surface salinity and wind retrieval. *Journal of Geophysical Research: Oceans*, 119(8): 5360–5379, doi: [10.1002/2014JC009939](https://doi.org/10.1002/2014JC009939)